Supplementary information - Strongly nonlinear nanocavity exciton-polaritons in gate-tunable monolayer semiconductors

Wang et al.

1. Device fabrication

Figure S1 illustrates the flow of photonic device fabrication. We deposited a 150 nm-thick Si_3N_4 layer on a thermal oxide silicon wafer with a 450 nm-thick oxide layer using LPCVD. The photonic devices were defined on the Si_3N_4 layer using electron-beam lithography (Raith EBPG 5200ES) followed by reactive ion etching (Oxford 80 Plus). Subsequently, a 5/40 nm-thick of Cr/Au was deposited as metal contacts using a laser writer (Heidelberg DWL 66+) and e-beam evaporator. To suspend the nanobeam cavities and grating couplers, we utilized a 49% HF solution to etch the oxide layer beneath the patterned Si_3N_4 layer.

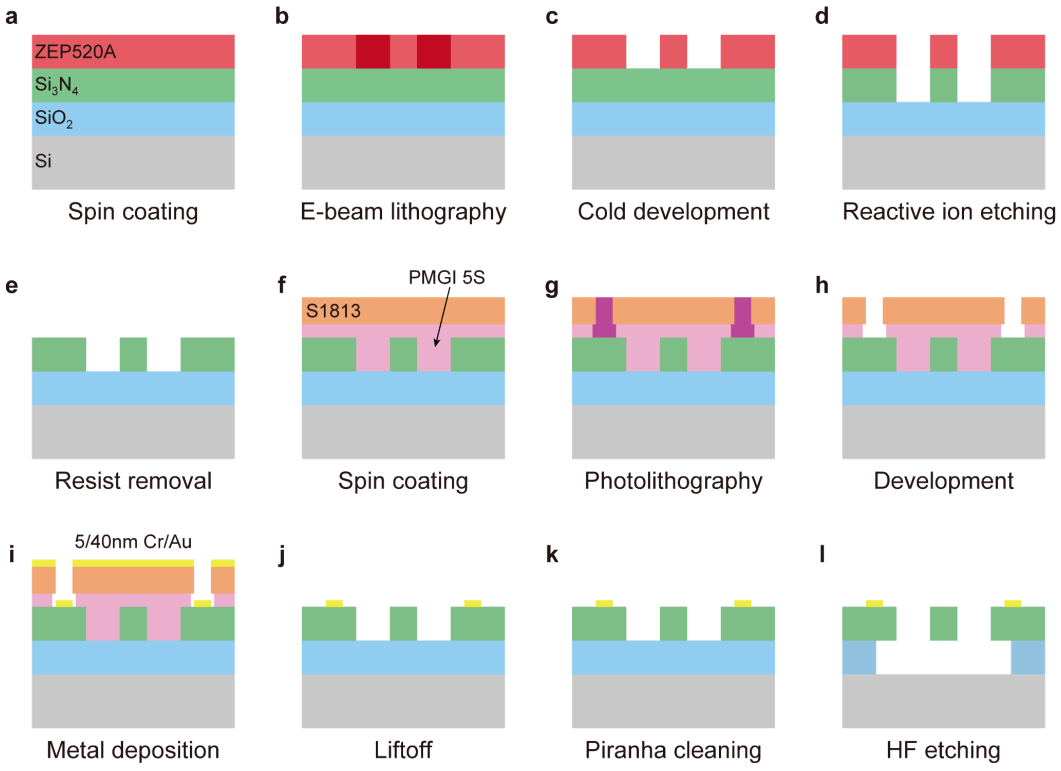

Supplementary figure 1. Flow chart of the fabrication process

$MoSe_2$ and WS_2 monolayers were mechanically exfoliated from CVT bulk crystals (HQ Graphene). Subsequently, these flakes were stacked and transferred onto the suspended nanobeam cavity using a standard dry transfer method. The graphite flakes were carefully aligned with the pre-patterned metal electrodes to facilitate electrostatic gating.

2. Photonic crystal nanocavity design

The photonic crystal nanobeam cavities are defined by adiabatically varying the lattice constant of the 1D array of air holes (diameter = 170 nm) from 228 nm at the center to 266 nm at both ends of the taper section (Fig. S2a). This variation ensures a Gaussian-like optical mode profile, leading to negligible radiative loss into free space. Furthermore, in the mirror section, four holes are employed to confine the cavity resonances while maintaining finite coupling with the waveguides on both sides (waveguide width w = 520 nm). The number of holes in the mirror section is carefully designed such that the radiative decay rate through the waveguides is comparable to the exciton decay rates. This design allows for efficient excitation and probe of polariton modes through bus waveguides.

The cavity resonances and mode profiles were calculated using the Finite Element Method (COMSOL Multiphysics 6.1). The simulated bare cavity exhibits an optical resonance at 1.718 eV with a quality factor of 3313. Upon introducing a 20 nm-thick hBN layer (ε_{BN} = 4.41), the optical resonance shifts to 1.658 eV. The quality factor decreases to 1628 due to a reduction in the photonic band gap, which leads to increased coupling with the waveguides. The predicted 60 meV redshift in the optical resonance aligns well with our experimental observation (Fig. S2b), where the cavity resonance shifts from 1.736 eV at room temperature to 1.656 eV at 4 K in the presence of the TMD stack. It is noteworthy that the measured quality factor of 166 at low temperature is lower than the numerical prediction. This deviation is attributed to the optical absorption near the exciton resonances in the $MoSe_2$ monolayer – a factor not accounted for in the simulation.

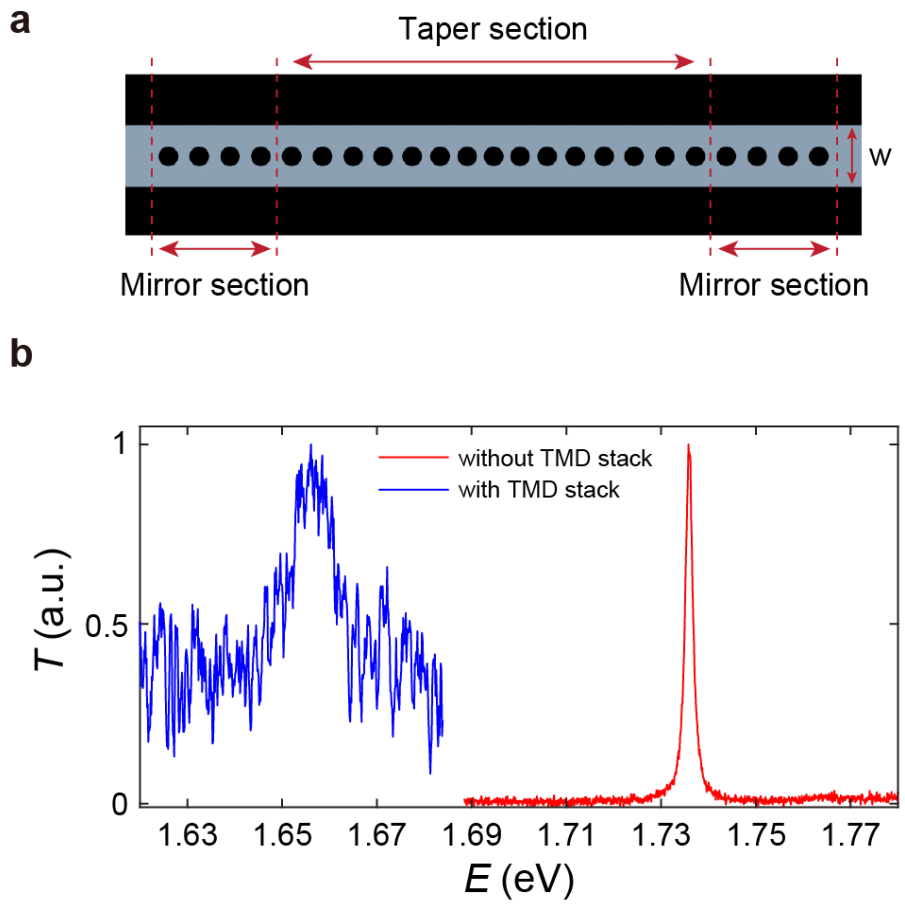

Supplementary figure 2. (a) Schematic of the photonic crystal nanobeam cavity. (b) Measured cavity transmission spectra with (blue) and without (red) TMD stack..

The nanocavity resonance is observed to drift gradually over time when the device is cooled to 4 K, presumably due to reduced mechanical stability of the suspended structure. For example, Fig. S3 shows bare cavity transmission spectra measured from the same device at three different times after cooldown. During the first 5 hours, the resonance gradually redshifts by 2 meV. Over the following 6 hours, it exhibits an additional redshift of approximately 1.9 meV. To mitigate this effect during the polariton nonlinearity measurements, all data were acquired within a 2-hour window, during which the resonance drift remained negligible.

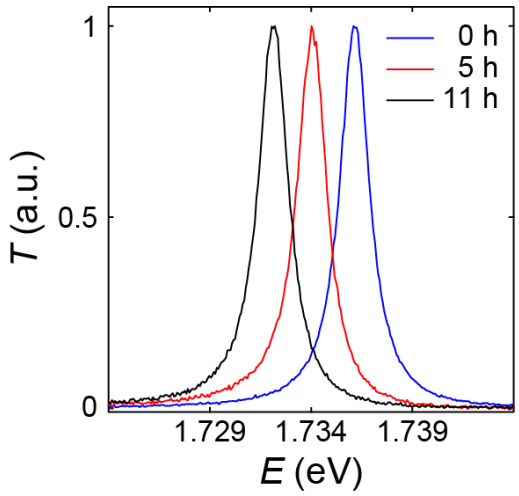

Supplementary figure 3. Transmission spectra of the bare cavity measured at 0 hours (blue), 5 hours (red), and 11 hours (black) after cooldown.

3. Slow recovery of the cavity spectrum

Figure S4 presents the pump-probe spectroscopy of nonlinear cavity polaritons, similar to the measurement shown in Fig. 4a of the main text, but extended to much longer time delays – up to 240 ps. We observe that the cavity spectrum requires at least several hundred picoseconds to fully recover to its equilibrium state. This recovery time is significantly longer than the exciton lifetime, which is on the order of a few picoseconds, suggesting the generation of other long-lived excitations in the system, such as in-gap states. Further investigation is required to clarify the origin of these slow relaxation dynamics.

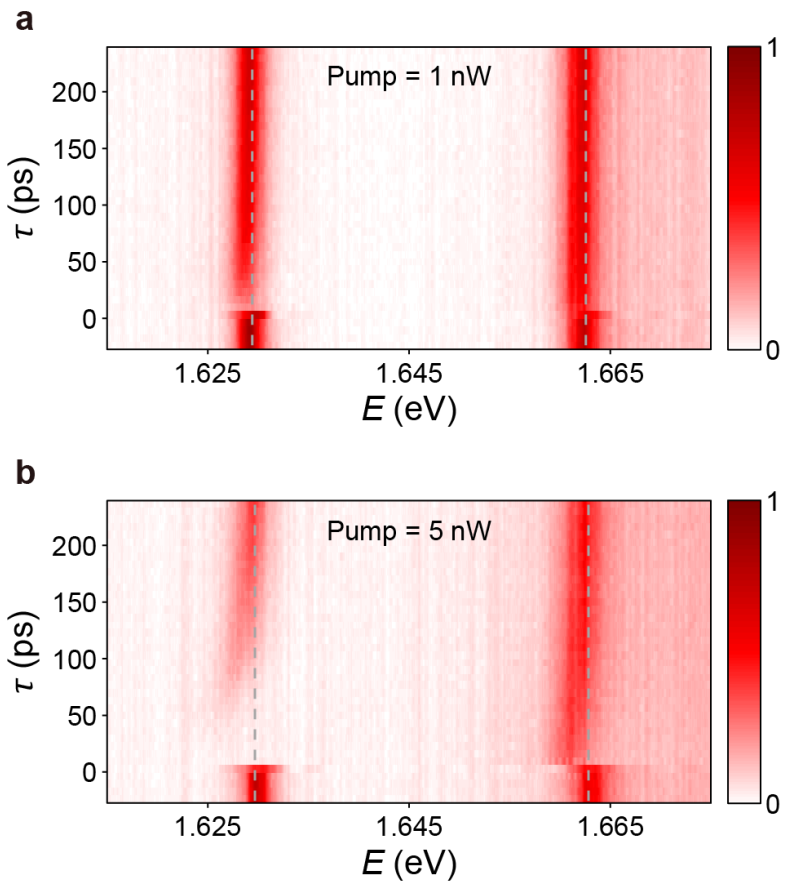

Supplementary figure 4. Pump-probe spectroscopy of nonlinear cavity polaritons at extended time delays.